Journal of Simulation and Analysis of Novel Technologies in Mechanical Engineering
17 (3) (2025) 0005~0010
DOI 10.71939/jsme.2025.1209757

Research article

A study on the effect of Sic particle distribution on the creep behavior of variable-thickness plates composed of functionally graded materials (FGMs)

Majid Amiri[1]*, Ahmad Keshavarzi[2]

[1]*Faculty of Mechanics, Malek Ashtar University of Technology, Isfahan, Iran*

[2]*Department of Mechanical Engineering, Khomeinishahr Branch, Islamic Azad University, Isfahan, Iran*

*majid.amiri@mut-es.ac.ir

(Manuscript Received --- 12 June 2025; Revised --- 02 Aug. 2025; Accepted --- 19 Aug. 2025)

Abstract

This paper investigates the creep behavior of a variable-thickness rectangular plate reinforced with silicon carbide (SiC) particles dispersed within an aluminum (Al) matrix. The distribution of SiC particles varies along the plate's thickness, and the structure is subjected to constant mechanical loading and non-uniform thermal loading, modeled as a linear temperature gradient through the thickness. The Classical Plate Theory is employed to derive the governing equations incorporating creep deformation, considering that both mechanical and thermal properties vary as functions of the local SiC volume fraction. To analyze creep behavior, Mendelson's successive approximation method combined with the Prandtl–Reuss constitutive equations is used. The resulting system of equations is solved using the Differential Quadrature Method (DQM). The study aims to evaluate different reinforcement distribution profiles to identify the optimal configuration in terms of failure criteria and long-term creep displacement. Specifically, the plate's creep response is examined for various SiC distributions with an average volume fraction of 25% over a 5-year period.

Keywords: Creep, Silicon Carbide, FGM materials, Variable thickness.

1- Introduction

Time-dependent deformation is referred to as creep, a process that occurs slowly under a constant load. This phenomenon is also temperature-dependent, with the creep rate increasing as temperature rises. The most critical temperature for the onset of significant creep is approximately 0.4 times the melting point of the material, beyond which creep becomes considerable. Creep leads to a change in material behavior from isotropic to anisotropic, deformation, strength reduction, and potentially serious damage to structural components. Therefore, studying creep behavior is essential and unavoidable.

While many studies have focused on creep in cylinders and disks, limited research has addressed creep in plates. Creep in rotating disks made of Al–SiC functionally graded materials (FGMs) was investigated by Singh and Rai [1]. Loghman and Wahab studied creep damage in thick-walled pipes using the theta projection creep model and Mendelson's successive approximation method [2]. Creep damage in thick-walled

spheres was analyzed by Loghman and Shokoohi [3], and Loghman et al. [4] also investigated the time-dependent stress history in FGMs cylinders subjected to internal and external pressure, temperature, and magnetic fields. Time-dependent creep in thick walled steel cylinders was semi-analytically studied by Loghman and Moradi [5]. Creep behavior of FGMs cylinders under asymmetric loading was examined by Arefi et al. [6], who applied a semi-analytical method and Norton's creep model. Using First-Order Shear Deformation Theory (FSDT), Loghman et al. [7] analyzed time-dependent creep in thick-walled FGMs cylinders via the analytical Young method. Zarifi and Akhlaghi [8] analyzed the creep behavior of rotating FGMs disks using the Sherby's creep model. Creep analysis of variable-thickness beams was conducted by Mirzaei et al. [9] using Sherby's model and Mendelson's elastic successive approximation method to obtain stress and displacement histories. There are very few studies concerning creep in plates. Notably, Vladimir et al. [10] investigated creep in polymeric plates. Amiri et al. [11] investigated thermoelastic analysis of rectangular plates with variable thickness made of FGM based on TSDT using DQ method. They also analyzed Creep analysis of plates made of functionally graded Al-SiC material subjected to thermomechanical loading [12].

2- Modeling, loading, and temperature distribution

The variable-thickness thin plate is subjected to both thermal and mechanical loading. The mechanical load is uniform, while the thermal load varies linearly along the thickness, such that the temperature at each point is constant through the plate's plane but changes along the thickness direction (see Fig. 1). The coordinate system is positioned at the mid-plane of the rectangular plate, and the plate is assumed to have fixed boundary conditions. Fig. 2 illustrates the temperature distribution function along the thickness direction of the plate.

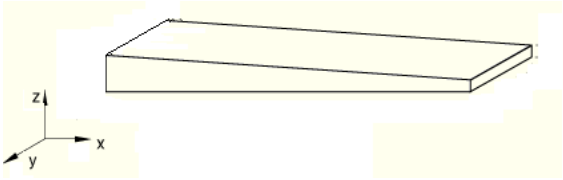

Fig. 1 Plate with variable thickness along the x-direction (thickness increasing with x)

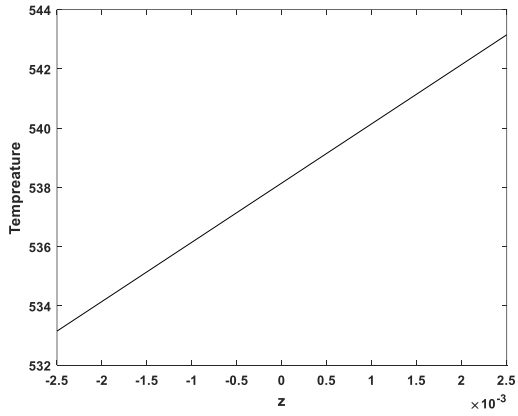

Fig. 2 Linear temperature distribution as a function of thickness

3- Geometric dimensions, loading, and diagrams

The variation of thickness is also assumed to be a linear function of x, increasing in that direction. The geometric dimensions, loading conditions, and other properties of the plate considered for creep analysis are as follows:

$$
\begin{aligned}
&a=b=1\ (m),\quad h=0.006,\quad Q=100\ KN\\
&E_{Al}=70Gpa,\quad E_{sic}=410Gpa,\quad K_{Al}=237Wm^{-1}c^{-1}\\
&K_{sic}=120Wm^{-1}c^{-1},\quad \nu=0.30,\quad \alpha_{Al}=23.1\times10^{-6}K^{-1}\\
&\alpha_{sic}=4\times10^{-6}K^{-1},\quad T_{min}=260^{0}C,\quad T_{max}=270^{0}C\\
&\sigma^{*}=\frac{\sigma}{E_{Al}},\quad W^{*}=\frac{W}{a}\\
&h=h_{0}\left(1+\zeta\frac{x}{a}\right)\quad \zeta=0.1
\end{aligned}
\tag{1}
$$

4- Effect of SiC Particle Distribution on Creep

In this section, the effect of the distribution pattern of SiC particles within the Al matrix on creep is investigated. The average volume fraction of SiC particles in the aluminum matrix is denoted by C_{avg}. The creep behavior of the plate is studied under four different combinations of C_{min} and C_{max}, all maintaining an average volume fraction of 25%.

5- Calculation of C_{min} Based on C_{max} and C_{avg}

The distribution of silicon carbide reinforcement follows a linear variation from the bottom to the top surface of the plate, described by Equation (2): [13]

$$C(z) = C_{\min} + (C_{\max} - C_{\min}) V_c$$
$$V_c = \frac{z}{h} + \frac{1}{2} \quad (2)$$

C(z) represents the distribution of silicon carbide particles along the thickness direction z. $C_{\max}$ and $C_{\min}$ are the volume fractions of SiC at the top and bottom surfaces of the plate, respectively, and their values range between 0 and 1. The mechanical and thermal properties of the functionally graded material (FGM), excluding the Poisson's ratio, are functions of the SiC distribution and are expressed as follows:

$$P(z) = P_{Al} + (P_{SiC} - P_{Al}) C(z) \quad (3)$$

P(z) includes all material properties (excluding Poisson's ratio), where PAL and $PSiC$represent the properties of aluminum and SiC, respectively. P(z) includes elastic modulus, thermal conductivity, and coefficient of thermal expansion. For example, for the elastic modulus:

$$E(z) = E_{Al} + (E_{SiC} - E_{Al}) C(z)$$
$$E(z) = E_{Al} + (E_{SiC} - E_{Al}) C(z) \quad (4)$$
$$E(z) = E_{Al} + (E_{SiC} - E_{Al}) ....$$
$$... \left[C_{\min} + (C_{\max} - C_{\min}) \left(\frac{z}{h} + \frac{1}{2} \right) \right]$$

The Poisson's ratio is considered constant due to its relatively small effect on deformation compared to Young's modulus.

First, the average thickness of the plate is calculated:

$$h(x) = h_0 (1 + \alpha x)$$
$$h_{avg} = \frac{1}{a} \int_0^a h(x) dx = \frac{1}{a} \int_0^a h_0 (1 + \alpha x) dx \quad (5)$$
$$= h_0 (1 + \frac{\alpha}{2})$$

Since the plate width b is constant:

$$b \int_0^a \int_{-\frac{h(x)}{2}}^{\frac{h(x)}{2}} C(z) dz dx = b C_{avg} a h_{avg} \quad (6)$$

Continuing the calculations:

$$C_{avg} = \frac{1}{a h_{avg}} \int_0^a \int_{-\frac{h(x)}{2}}^{\frac{h(x)}{2}} C(z) dz dx = \frac{1}{a h_{avg}}$$
$$\int_0^a \int_{-\frac{h(x)}{2}}^{\frac{h(x)}{2}} \left(C_{\min} + \left((C_{\max} - C_{\min}) \left(\frac{z}{h} + \frac{1}{2} \right) \right) \right) dz dx = \quad (7)$$
$$\frac{1}{a h_{avg}} \int_0^a \int_{-\frac{h(x)}{2}}^{\frac{h(x)}{2}} \left(\left(\frac{C_{\max} + C_{\min}}{2} \right) + \left((C_{\max} - C_{\min}) \left(\frac{z}{h} \right) \right) \right)$$
$$dz dx = \frac{h_0}{h_{avg}} \left(\frac{C_{\max} + C_{\min}}{2} \right) \left(1 + \frac{\alpha a}{2} \right)$$

Substituting h_{avg} from Equation (5) into Equation (7):

$$C_{avg} = \frac{h_0}{h_{avg}} \left(\frac{C_{\max} + C_{\min}}{2} \right) \left(1 + \frac{\alpha a}{2} \right) = \quad (8)$$
$$\left(\frac{C_{\max} + C_{\min}}{2} \right) \frac{\left(1 + \frac{\alpha a}{2} \right)}{\left(1 + \frac{\alpha}{2} \right)}$$

By evaluating Equation (8) with respect to C_{min}:

$$C_{\min} = \frac{2(2+\alpha)C_{avg} - (2+\alpha a)C_{\max}}{(2+\alpha a)} \quad (9)$$

In the above equation, C_{min} is obtained as a function of C_{max}, C_{avg}, a, and α. Based on the above relationships, the values in Table (2) are derived:

Table 1: Creep behavior analysis for different C_{max} and C_{min} values

C_{max}	25%	30%	35%	40%
C_{min}	25%	20%	15%	10%
C_{avg}	25%	25%	25%	25%

For creep displacement analysis, both Mendelson's method and the DQM (Differential Quadrature Method) were used.

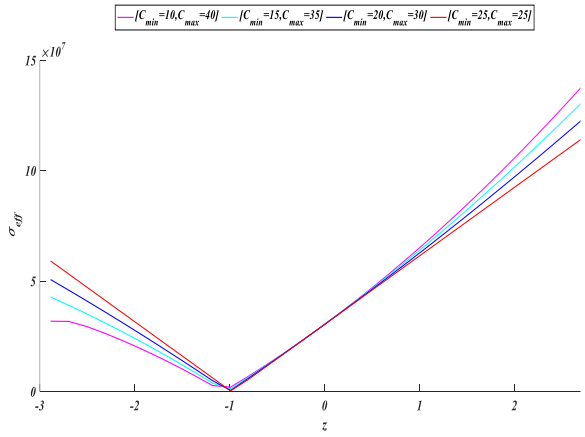

Fig. 3 Effective stress diagram at different volume fraction ratios at the initial time (C_{avg} = 25%)

Figs. (3) and (4) show the effective stresses at the initial time and after 5 years, respectively. Based on the graphs and the Tresca criterion, the case where C_{min} and C_{max} are both 25% performs better than other conditions.

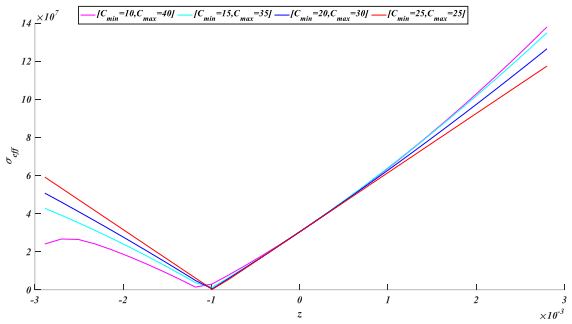

Fig. 4 Effective stress diagram at different volume fraction ratios after 5 years (C_{avg}= 25%)

Subsequently, a comparison is made between the initial and long-term creep displacements for different volume fraction ratios after 5 years. Except for the case with C_{min}= 0.10 and C_{max}= 0.40, the displacements in other scenarios are negligible.

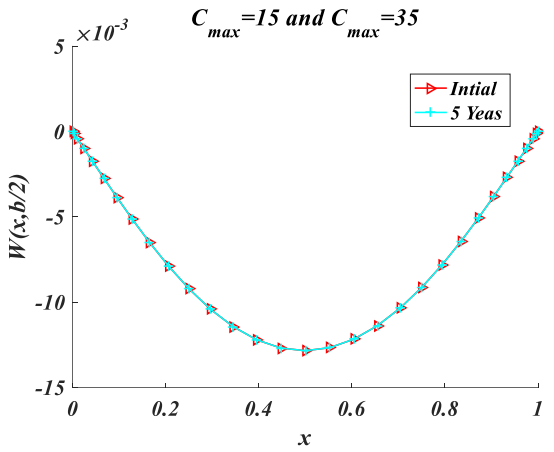

Fig. 5 Initial and creep displacements after 5 years for the case (C_{min}=15, C_{max}=35 and C_{avg}= 25%)

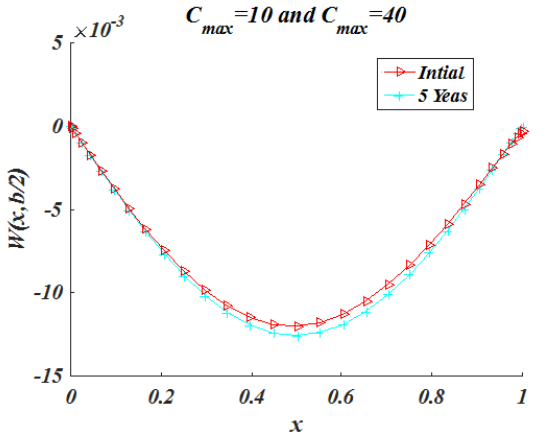

Fig. 6 Initial and creep displacements after 5 years for the case (C_{min}=10, C_{max}=40 and C_{avg}= 25%)

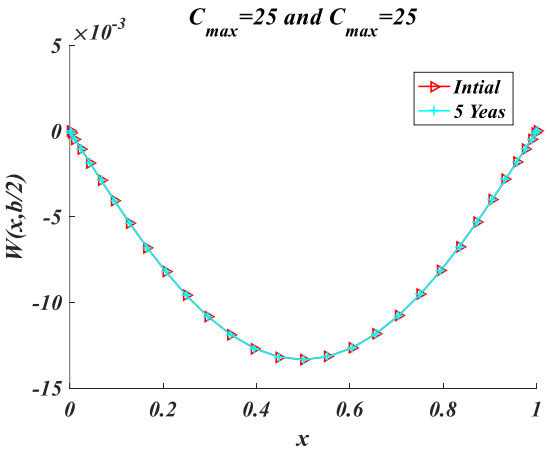

Fig. 7 Initial and creep displacements after 5 years for the case (C_{min}=25, C_{max}=25 and C_{avg}= 25%)

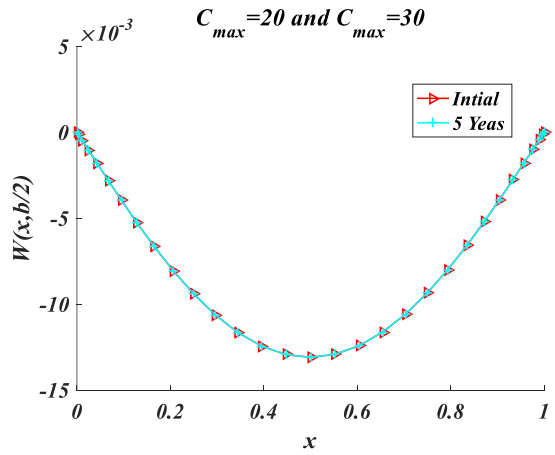

Fig. 8 Initial and creep displacements after 5 years for the case (C_{min}=20, C_{max}=30 and C_{avg}= 25%)

6- Conclusions

This study examined the creep behavior of a plate with variable thickness concerning the distribution of SiC particles. The creep displacement of the plate was evaluated after five years under different volume fraction ratios. According to the Tresca criterion, a smaller variation in effective stress through the thickness corresponds to higher strength, which occurs when both the maximum and minimum volume fractions are equal to 25%. Additionally, a comparison of creep displacements for various volume fraction ratios after 5 years showed that, except for the case where $C_{min} = 0.10$ and $C_{max} = 0.40$, the displacements in other cases are negligible.

References

[1] Loghman, A. and Wahab, M. A. (1996). Creep damage simulation of thick-walled tubes using the Θ projection concept. *International Journal of Pressure Vessels and Piping*, 67 (1) 105-111.

[2] Singh, S.B. and Ray, S. (2003). Creep analysis in an isotropic FGM rotating disk of Al–SiC composite, *Journal of Materials Processing Technology*, 143-144 616–622.

[3] Loghman, A. and Shokouhi, N. (2009). Creep damage evaluation of thickwalled spheres using a long-term creep constitutive model. *Journal of Mechanical Science and Technology*, 23, 2577-2582.

[4] Loghman, A., Ghorbanpour Arani, A., Amir, S. and Vajedi, A. (2010). Magnetothermoelastic creep analysis of functionally graded cylinders. *International Journal of Pressure Vessels and Piping*, 87(7), 389-395.

[5] Moradi, M. and Loghman, A. (2018). Non-Axisymmetric TimeDependent Creep Analysis in a Thick-Walled Cylinder Due to the Thermo-mechanical loading. *Journal of Solid Mechanics*, 10(4), 845-863.

[6] Arefi, M., Nasr, M. and Loghman, A. (2018). Creep analysis of the FG cylinders: Time-dependent non-axisymmetric behavior. Steel and Composite Structures, 28(3), 331-347.

[7] Loghman, A., Koohi Faegh, R. and Arefi, M. (2018). Two dimensional time-dependent creep analysis of a thick-walled FG cylinder based on first order shear deformation theory. Steel and Composite Structures, 26(5), 533-547.

[8] Zharfi, H., Ekhteraei Toussi, H. (2017). Numerical creep analysis of FGM rotating disc with GDQ method. *Journal of theoretical and applied mechanics,* 55(1), 331-341.

[9] Mirzaei, M.M.H, Arefi, M and Loghman, A. (2019). Time-dependent creep analysis of a functionally graded simple blade using first-order shear deformation theory. *Australian Journal of Mechanical Engineering*, 448-4846, 2204-2253.

[10] Vladimir A., Yazyev, B.M. and Chepurnenko A. (2014). On the Bending of a Thin Plate at Nonlinear Creep. *Advanced Materials Research*, 900,707-710.

[11] Majid Amiri, Abbas Loghman, Mohammad Arefi, (2023). Thermoelastic analysis of rectangular plates with variable thickness made of FGM based on TSDT using DQ

method. *Geomechanics & engineering*. 29 (6), 667-681.

[12] Majid Amiri, Abbas Loghman, Mohammad Arefi, (2023). Creep analysis of plates made of functionally graded Al-SiC material subjected to thermomechanical loading. *Advances in concrete construction*. 15 (2), 115-126.

[13] Golmakaniyoon, S. and Akhlaghi, F. (2016). Time-dependent creep behavior of Al–SiC functionally graded beams under in-plane thermal loading. *Comput. Mate. Sci*., 121, 182–190.